Semiconductor Science and Technology

ACCEPTED MANUSCRIPT • OPEN ACCESS

Single event burnout sensitivity of SiC and Si

To cite this article before publication: Matthew Thomas Michael Littlefair *et al* 2022 *Semicond. Sci. Technol.* in press https://doi.org/10.1088/1361-6641/ac668c

Manuscript version: Accepted Manuscript

Accepted Manuscript is “the version of the article accepted for publication including all changes made as a result of the peer review process, and which may also include the addition to the article by IOP Publishing of a header, an article ID, a cover sheet and/or an ‘Accepted Manuscript’ watermark, but excluding any other editing, typesetting or other changes made by IOP Publishing and/or its licensors”

This Accepted Manuscript is **© 2022 The Author(s). Published by IOP Publishing Ltd.**.

As the Version of Record of this article is going to be / has been published on a gold open access basis under a CC BY 3.0 licence, this Accepted Manuscript is available for reuse under a CC BY 3.0 licence immediately.

Everyone is permitted to use all or part of the original content in this article, provided that they adhere to all the terms of the licence https://creativecommons.org/licences/by/3.0

Although reasonable endeavours have been taken to obtain all necessary permissions from third parties to include their copyrighted content within this article, their full citation and copyright line may not be present in this Accepted Manuscript version. Before using any content from this article, please refer to the Version of Record on IOPscience once published for full citation and copyright details, as permissions may be required. All third party content is fully copyright protected and is not published on a gold open access basis under a CC BY licence, unless that is specifically stated in the figure caption in the Version of Record.

View the article online for updates and enhancements.

This content was downloaded from IP address 129.234.39.251 on 20/04/2022 at 14:24

Single Event Burnout Sensitivity of SiC and Si

Matthew T M Littlefair[1], **Sergei Simdyankin**[1], **Simon Turvey**[2], **Chris Groves**[1] **and Alton B Horsfall**[1]

[1] Department of Engineering, University of Durham, Durham, DH1 3LE, United Kingdom

[2] Rolls-Royce, Derwent Building, Birmingham, B37 7YP, United Kingdom

E-mail: `matthew.littlefair@durham.ac.uk`, `sergei.simdyankin@durham.ac.uk`, `simon.turvey@rolls-royce.com`, `chris.groves@durham.ac.uk` and `alton.b.horsfall@durham.ac.uk`

Abstract. Exposure to ionizing radiation has the potential to catastrophically modify the operation, and destroy, electronic components in microseconds. The electrification of aircraft necessitates the need to use the most power dense and lowest loss semiconductor devices available, and the increasing supply voltages results in extremely high electric fields within the devices. These conditions create the worst case environment for the Single Event Effect (SEE), the instantaneous alteration in device response after high energy particle interaction, with a destructive form of SEE, the Single Event Burnout (SEB), resulting in total failure of the device with potentially explosive consequences. To enable circuits to operate with these high supply voltages, SiC is rapidly becoming the semiconductor of choice. However, the radiation response of SiC power devices during operation is unknown. Here we show that SiC offers a 60% reduction in cosmic ray sensitivity in comparison to Si devices with an equivalent voltage rating. The data show that Si fails when subjected to a heavy ion impact with Linear Energy Transfer (LET) equivalent to 0.2% of the silver ions commonly used for Single Event Effect testing. In total contrast, we show that SiC does not exhibit failure during exposure to any heavy ion LET up to values three times greater than those commonly used in testing at any bias up to 99% of the breakdown voltage. The data show that SiC is a robust material and therefore has the potential to replace Si as the material of choice for high reliability avionic applications, as it far exceeds the performance of Si in cosmic ray environments, facilitating significant advances in the electrification of aircraft to be made in the near future.

Keywords: SiC, Radiation Effects, Single Event Burnout, Single Event Effects

1. Introduction

With the global challenge to achieve Net-Zero by 2050, aviation, a significant contributor to the generation of greenhouse gas emissions, producing 900 million tonnes of CO_2 emissions annually, is committed to a step change in propulsion technology. The electrification of aircraft is considered to be the most realistic strategy to achieve the required significant CO_2 reductions by utilizing all electric, hybrid electric and zero carbon power systems. Realization of these MW scale power systems will rely on the incorporation of wide bandgap semiconductors, such as silicon carbide (SiC) – a semiconductor with excellent material properties, including critical electric field strength, high electron saturation drift velocity and high thermal conductivity. The superior properties of SiC are required to make this goal a reality through offering the ability to operate at power levels significantly beyond those of traditional silicon (Si). However, at the current time, knowledge of the interaction of cosmic ray radiation with power electronic devices manufactured from SiC is unknown, limiting their use in aerospace applications. For computing electronics, testing and mitigating solutions for single event upset are well established practices. However, ionizing radiation effects for power devices will require mitigation solutions beyond voltage de-rating which have not yet been established.

The cumulative long term damage to the semiconductor lattice that results from the interaction between the atoms in the lattice and the high energy particles generated from solar events is generally described using Total Ionizing Dose (TID) and Displacement Damage (DD). Radiation has been shown to cause leakage current degradation and increased power dissipation in the electronic devices that are required to support more electric aircraft [1] and the literature show that the radiation response of SiC to cumulative damage is superior to that of Si [2]. However, the instantaneous response of devices caused by the interaction with the high energy particles can result in catastrophic failure [3], which is the focus of the work reported here.

A Single Event Effect (SEE) occurs when an ionizing particle interacts with the atoms within an electronic device, depositing charge and hence shifting the operating conditions away from equilibrium in a ns timescale. The deposited charge is in the form of a trail of electron hole pairs (ehps). If the device is in the blocking state, the ehps can multiply in regions of high electric field and generate an avalanche of charge – resulting in temperature hotspots in excess of 2000 K and thermal runaway, where device explosion can be a consequence if insufficient quenching measures exist [4]. Single Event Burnout (SEB) is a destructive form of SEE and clearly has the potential to disrupt power electronic systems exposed to radiation – one of the most notable being the aerospace sector. To mitigate these potentially catastrophic failures in aerospace applications, system level redundancy is a proven method. However, the influence of a SEB on a power electronic component that forms part of the propulsion system for an aircraft has the potential to be life threatening. At commercial flight altitudes the flux of incident particles originating from cosmic rays is approximately 1000 times greater than at sea level, placing global pressure on the inclusion of SEE and SEB hardness assurance certification for avionics. If a power electronic device were to suffer an impact with a high energy cosmic ray particle when operating in the blocking state, where the internal electric field is close to the critical electric field of the semiconductor, the consequences could be catastrophic - device explosion and potential system failure. The critical electric field, the maximum electric field that a material can support before suffering physical breakdown and unsupported current flow, in SiC is an order of magnitude higher than that in Si, which enables the reduction in on–state resistance of power electronic devices, leading to enhanced efficiencies. In this work, thin devices are simulated and therefore the the definition of critical electric field cannot be applied in the same way that it is with thicker devices, rather, it is an indication of the severity of the influence of the heavy ion impact on the material response. Regardless of the material, when charge carriers are generated through the device due to ionizing radiation, additional carriers will be generated in regions of high electric field due to avalanche multiplication processes, with a higher electric field resulting in a greater number of carriers.

The literature has reported on the SEB sensitivity of Si power devices [5]. Casey *et al.* irradiated commercially sourced Si power Schottky diodes held at a range of reverse bias voltages and operating at different forward currents, with a 1233 MeV Xe ion beam. The findings showed that devices operated with reverse bias voltages below 50% of the specified rating are unlikely to undergo SEB failure. Initial research on the SEB sensitivity of SiC devices has also been reported [6]. The data demonstrated evidence of device failure resulting from SEB after exposure to ion LETs as low as 3 MeV-cm^2/mg, (0.02 pC/μm) when the reverse bias was held at values greater than

65% of the device rated voltage. Data published by Lauenstein *et al.* reported that SiC devices show evidence of SEB related failures when the reverse bias is 30% of the specified breakdown voltage for the lowest LET value studied.

The unique benefit of having performed simulations over physical testing in this work is that true SEB data are produced as there is no influence from prior heavy ion strikes which are typical in heavy ion beam testing. However, there has not been a systematic study in which SEB sensitivity has been measured for equivalent Si and SiC devices under equivalent LET conditions. Hence, the question of materials choice for power electronics used in propulsion systems for aircraft is unclear. Systematically for the first time the material response of Si and SiC p–i–n diodes from single heavy ion impacts, with energies matching those of cosmic rays that are relevant in aerospace environments, have been investigated. Here, the generated charge from the cosmic ray induced current transients have been analyzed to identify the respective material SEB sensitivity. From this, the optimal operating conditions for both devices in real world avionic applications was determined. Further, a key emphasis has been placed on understanding the transient response of the collected charge within the device, as this enables the determination of the physics of failure for both Si and SiC. As a consequence, our systematic study has demonstrated the improved SEB resilience of SiC devices as compared to Si in aerospace applications.

The paper is structured as follows: in section 2, detail of the simulated structures and models used in this work are described, section 3 provides a comparative study of SiC and Si devices under the influence of a range of aerospace specific operating conditions, and conclusions are presented in section 4.

2. Simulations

Our approach was to focus on the influence of the material properties on the SEE characteristics and therefore a simple p–i–n structure was selected. To ensure consistent breakdown voltages of the diodes different intrinsic region thicknesses were selected at 40.0 μm and 5.0 μm for the Si and SiC devices respectively. Systems used in the electrification of aircraft use the breakdown voltage of devices as a benchmark, and for this reason, this parameter has been selected over matching the device structures for this comparative study of Si and SiC. The schematic of both the Si and the SiC PiN

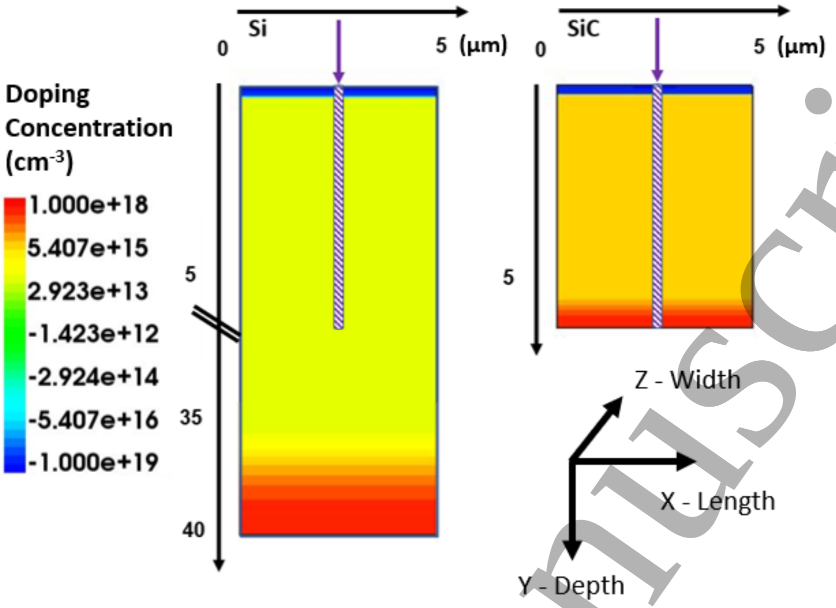

Figure 1. Si and SiC device structures with the simulated heavy ion tracks and impact locations.

Table 1. TCAD simulation parameters used in this study.

Parameter	4H-SiC	Si
Material Bandgap	3.23 eV [7]	1.12 eV [8]
Density	3211 mg/cm^3 [9]	2328 mg/cm^3 [10]
Ion pair generation energy	7.8 eV [11]	3.6 eV [12]
Critical Electric Field	2.07 MV/cm	0.24 MV/cm
P+ Doping/Depth	10^{19}cm^{-3}, 0.25 μm	10^{19}cm^{-3}, 0.25 μm
N-Epi Doping/Depth	10^{16}cm^{-3}, 5.0 μm	10^{14}cm^{-3}, 40.0 μm
N+ Doping/Depth	10^{18}cm^{-3}, 1.0 μm	10^{18}cm^{-3}, 1.0 μm
Device Length	5.0 μm	5.0 μm
Device Width	1.0 μm	1.0 μm
Active Area	5.0 μm^2	5.0 μm^2

diode models can be seen in figure 1 and the relevant parameters are summarized in table 1. The breakdown voltage of the diodes was set to 868 V, as can be seen from the data in figure 2.

Here single heavy ion injection has been used to determine the response of Si and SiC devices to cosmic ray impacts. To gain an understanding of the performance of devices under the influence of cosmic rays, the Synopsys Sentaurus TCAD software [13] has

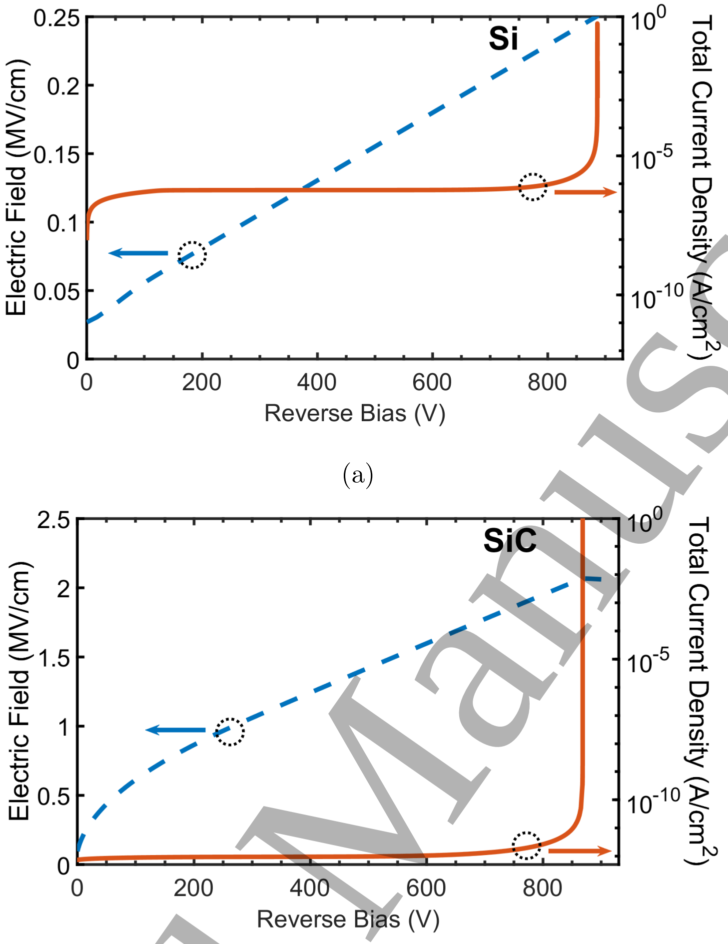

(a)

(b)

Figure 2. Breakdown of a 5 μm^2 device area (a) Si and (b) SiC PiN diodes at 300 K with parameters summarized in table 1. Please note that the electric field in (b) is 10 times greater than that of (a).

been used. The parameters used in the heavy ion model are summarized in table 2. For both device types the ambient temperature was set to 300 K and the surface resistance, a key parameter for the boundary conditions of the materials studied, was set to 0.005 cm^2 K/W. The heavy ion impact location has been selected to be perpendicular to the device as to maximize the heavy ion track length, leading to the worst case scenario for a given heavy ion Linear Energy Transfer (LET) [14]. The simulations performed in this work have an end time of 100 ns after initial heavy ion impact, a value which has been selected to match the switching time of similar power devices. When the device switches from the OFF-state to the ON-state it recovers from the heavy ion induced charge deposition and returns to normal operation.

Table 2. Parameters for the heavy ion model.

Parameter	Value
Track Radius ω_0	0.05 μm
Track Length	6.25 μm
Horizontal Ion Striking Position from origin	2.5 μm
Initial Charge Generation Time T_0	100 ps

This study focuses on the influence of a highly localized charge region on a device, based on the heavy ion model that is incorporated within the Sentaurus software. This model, rather than depositing small bursts of charge through the device, delivers a highly concentrated charge track, which replicates the electron – hole pairs formed by the incident radiation quanta. This condition can be considered as the most severe charge deposition condition, where the focus is on the correlation between the intrinsic material properties and the resulting SEE characteristics. The use of TCAD simulations allows the distribution of the internal electric field, impact ionization and current densities to be investigated at picosecond timescales to gain detailed understanding of the behaviour of the diode during the impact. This enables the determination of the response of each material to the same impact conditions and the physics of failure to be identified.

The purpose of these simulations was to observe the variation in response of the different semiconductor material types after cosmic ray impact. Hence, the heavy ion track length has been selected as 6.25 μm - the total depth of the SiC device. Here, an equivalent number of electron - hole pairs are generated in each material.

Simulations have been performed for reverse bias voltages ranging from 99% of the breakdown voltage, through to the industry standard derating of 70%, down to a few percent of breakdown. Most flights an aircraft traverse a range of altitudes from sea level to around 40,000 ft, and given that the cosmic ray flux depends on the altitude, a range of heavy ion impact energies have been simulated to obtain knowledge of the sensitivity of the different materials. The largest heavy ion LET used is three times greater than that of a silver ion with an energy of 46 MeV-cm^2/mg, which is commonly used for SEE testing [15].

In this work, the Okuto-Crowell avalanche model [16] has been selected for both device types. This model incorporates the dead space of the first carrier injected into the high-field region, and thus is more applicable to the current data than purely local models. However, we note that in all cases, the dead space (i.e. the distance travelled by each charge before ionization is possible) is a small fraction of the depletion region width, with dead space values of 0.04 μm and 0.18 μm for SiC and Si respectively with depletion region widths of 100 times the dead space. This model was originally proposed for narrow bandgap materials, however, it has since been adapted for SiC by extracting ionization coefficient parameters from photomultiplication experiments [17,18], whereas for Si the parameter values of the original work of Okuto-Crowell are used. The model coefficients have been calibrated up to 580 K [17], however we note that it is challenging to determine coefficients beyond this temperature. It would be expected that as temperature increases further, the ionization coefficients will continue to fall as a consequence of increased phonon scattering. Thus we have confirmed that the parametrization continues to reduce beyond 580 K, meaning that our predications of impact ionization behaviour in this temperature region are reasonable first order estimates. The α and β coefficients are the impact ionization coefficients for electrons and holes respectively, and are used to describe avalanche multiplication by representing the mean rate of ionization per unit distance for a carrier. These coefficients are highly dependent on the internal electric field, because carriers only gain sufficient energy to result in impact ionization in areas of high electric field [19].

The electric field and current density for the SiC and Si devices as a function of reverse bias are shown in figure 2. The resulting maximum electric fields are 2.07 MV/cm and 0.24 MV/cm respectively, which are of importance when referring to the transient electric field as will be discussed later in the paper.

3. Results and Discussion

The data in figure 3(a) and (b) show the electric field time evolution along a heavy ion track in both materials biased at 600 V an industry standard derating to 70% of the breakdown voltage. The simulations have been performed for a heavy ion impact following the parameters summarized in table 2 with a LET of 0.1002 pC/μm, which corresponds to a deposited charge of 0.626 pC. This LET value allows a direct comparison to those used in heavy ion beam physical testing as it has a similar order of magnitude to the LET of silver ions. It can be seen from the data in both figures that the internal electric field profile varies with time for both materials – playing a crucial role on the resulting current density and therefore the magnitude of collected charge at the device terminals. In both cases, the pre-strike electric field is trapezoidal which is to be expected in p–i–n structures. First we discuss the SiC data in figure 3(b). The 80 ps data show the behaviour when the heavy ion charge generation rate returns to 0 cm^{-3}s^{-1}, resulting in a uniform charge concentration being deposited. The transit of generated carriers to the terminals results in the formation of a 'hammock' profile with the anode peak exceeding the critical electric field leading to enhanced impact ionization. This sustains the current peak displayed in figure 4(b) for 0.1 ns. Referring to the SiC data in figure 3(b), due to the small drift region in SiC the electric field profile returns to pre-strike (overlapped) conditions within 150 ps. In contrast, the Si data in figure

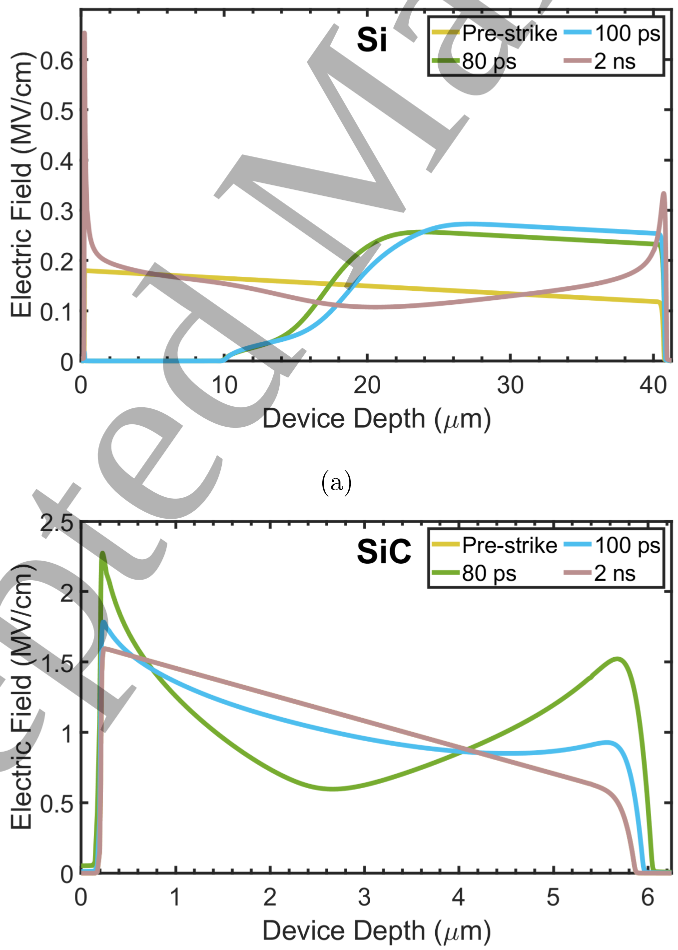

(a)

(b)

Figure 3. Electric field time evolution along a 0.1002 pC/μm LET and 6.25 μm track length heavy ion in (a) Si and (b) SiC, with both biased at 600 V.

3(a), at 80 ps, show the electric field profile maximum shifts from the p+/n- junction deeper into the device as a high concentration of charge is deposited in the first 6.25 μm of the device depth. A prolonged evolution of the electric field profile occurs due to both the smaller pre-strike electric field magnitude and deeper device depth, resulting in a larger carrier transit time. Between 100 ps and 2 ns the profile transforms from a shifted trapezoid to a 'hammock' profile with large electric field spikes observed at the device junctions leading to an elongated high current region as observed in figure 4(a), through enhanced impact ionization in these regions. The electric field profile returns to pre-strike conditions 50 ns after the heavy ion strike.

The total current density after heavy ion impact can be used to predict the ultimate failure of the device resulting from SEB. The data in figures 4(a) and (b) show the

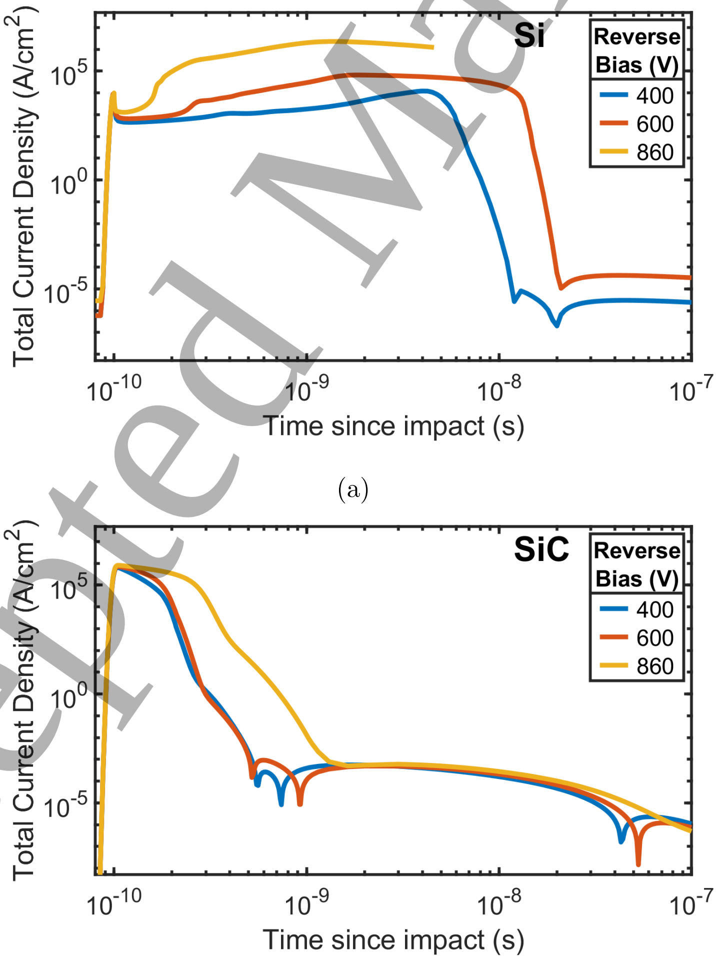

(a)

(b)

Figure 4. Ion-induced transient total current density for a heavy ion with 0.1002 pC/μm LET and 6.25 μm track length in (a) Si and (b) SiC.

transient current density of both device types after impact. For Si, the occurrence of a SEB is observed in the 860 V case, where the characteristics do not return to pre-strike conditions, which is defined here as a current density of approximately 1 μA/cm^2, 0.1 μs after impact. This contrasts with the behaviour of the 600 V and 400 V cases. The 600 V case is slower to return to equilibrium compared to the 400 V case as the magnitude of the electric field after impact is larger, leading to enhanced current generation over a longer time period. The initial current spike that can be observed in the data at the time of strike increases with increasing bias. A decay of the transient occurs over the next 5 ps, leading to growth towards the maximum value over the next 10 ns.

No indication of SEB is observed in the SiC data shown in figure 4(b). The total current returns to the pre-strike conditions even for the reverse bias of 860 V, 99% of the breakdown voltage. The initial spike in the current density for the SiC device is 50 times larger than that observed in the Si device and the duration increases with increasing reverse bias conditions. This initial spike implies the creation of a low resistance path between device terminals, in SiC which can be observed as a current peak that is sustained beyond the time at which the heavy ion charge generation rate returns to 0 cm^{-3}s^{-1}. The duration of this low resistance path is a potential issue when the device is used in a power electronic circuit, as the collected charge at the device terminals could exceed the critical charge to failure. The creation of a low resistance path is not observed in Si due to the drift region width being far greater than that of the heavy ion path length, rather, an increase in current density is observed primarily through impact ionization.

The ion-induced transient maximum temperatures for both material types are shown by the data in figures 5(a) and (b). For the Si device, contrasting behaviours are observed. At lower biases the maximum temperature peaks and then decays towards the initial pre-strike temperature, whereas, the 860 V data show thermal runaway, which peaks at 1687 K (not shown) which exceeds the melting point of Si [20]. In contrast, the SiC data show an increase in the maximum lattice temperature with increasing reverse bias, however this returns to the pre-strike temperatures in all cases examined here. The behaviour is due to the greater current in Si shown in figure 4(a).

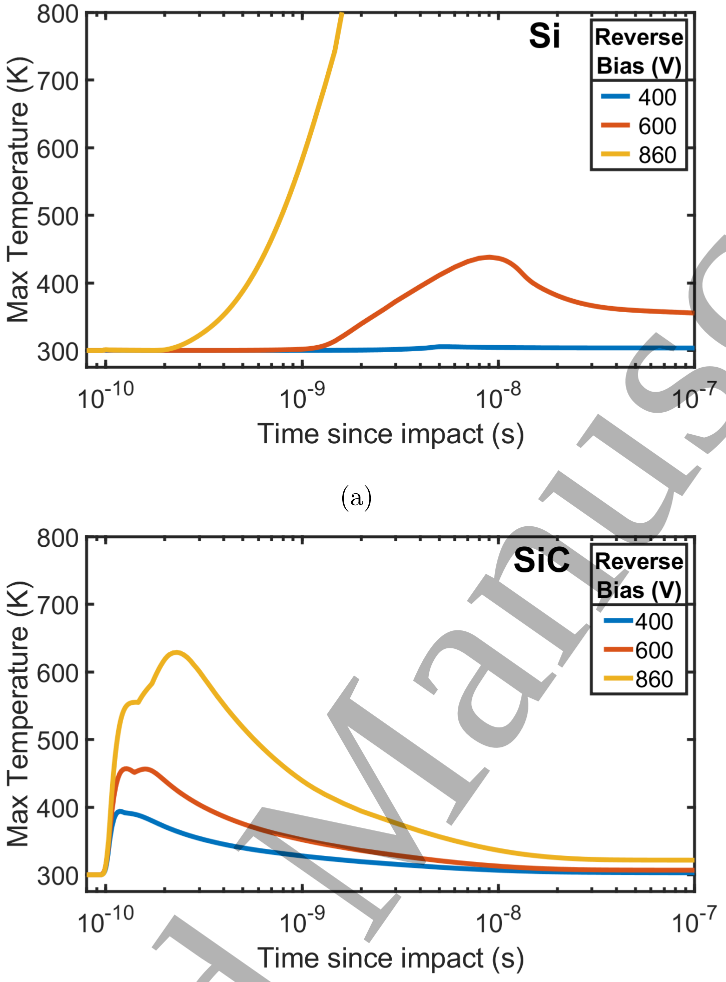

(a)

(b)

Figure 5. Ion-induced transient temperature for a heavy ion with 0.1002 pC/μm LET and 6.25 μm track length in (a) Si and (b) SiC.

We now turn to examine the total integrated charge collected following impact as a function of heavy ion deposited charges (equivalent to the LET in pC multiplied by the track length) to compare behaviours of the Si and SiC devices as shown by the data in figures 6(a) and (b). The total collected charge is determined by taking the integral of the current transients measured at the cathode contact for 100 ns after impact. For Si, figure 6(a), the data show the dependence of collected charge on applied voltage, with lower values of Q_{dep} requiring higher bias conditions to trigger multiplication which is in line with data in the literature [3]. As can be observed from the data, collected charge exceeding 400 pC indicates failure of the device - the lowest collected charge value to result in device melting. The data show that the failure of the device can be observed

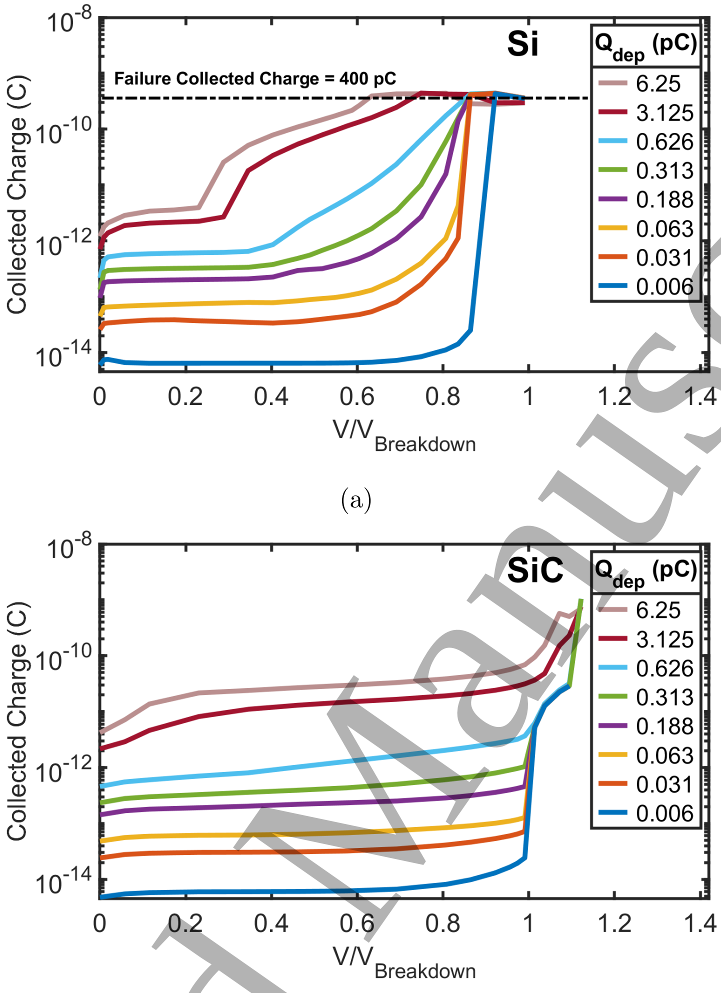

(a)

(b)

Figure 6. Collected Charge after heavy ion transient : (a) Si and (b) SiC.

below the breakdown voltage for heavy ion deposited charges as low as 0.006 pC (0.2% that of the silver ions commonly used in SEE testing) when a reverse bias of 800 V is applied. As the value of Q_{dep} increases, the voltage for which failure is observed reduces, such that for Q_{dep} of 6.25 pC, breakdown occurs at ∼60% of breakdown.

In SiC, it can be observed that a sharp jump in charge collected occurs at the breakdown voltage (as would be the case for no ionizing radiation) from Q_{dep} 0.006 pC to 0.626 pC. Hence, these simulations predict that SiC can operate at higher rated voltages even in the presence of a significant heavy ion impact. For all simulations performed on the SiC device no SEB failures occurred, and therefore, no value of failure collected charge had been identified.

We propose that the difference in behaviour between the two materials is due to the difference in how the electric field profiles vary after the strike, as shown in figure 3. Si shows significant enhancement of the electric field at the edges of the depletion region following the strike, figure 3(a), as compared to SiC, figure 3(b). To better understand this proposed effect, we now focus our attention on how the breakdown of devices are influenced by deposited charge. It can be seen from the data in figure 6 that collected charge increases with voltage due to charge multiplication. Therefore, in figure 7, we plot the voltage for which the different multiplication factors are observed as a function of deposited charge to allow for direct comparison between Si and SiC. Here, M is the ratio of the charge collected to the charge deposited in the device for Si and SiC diodes.

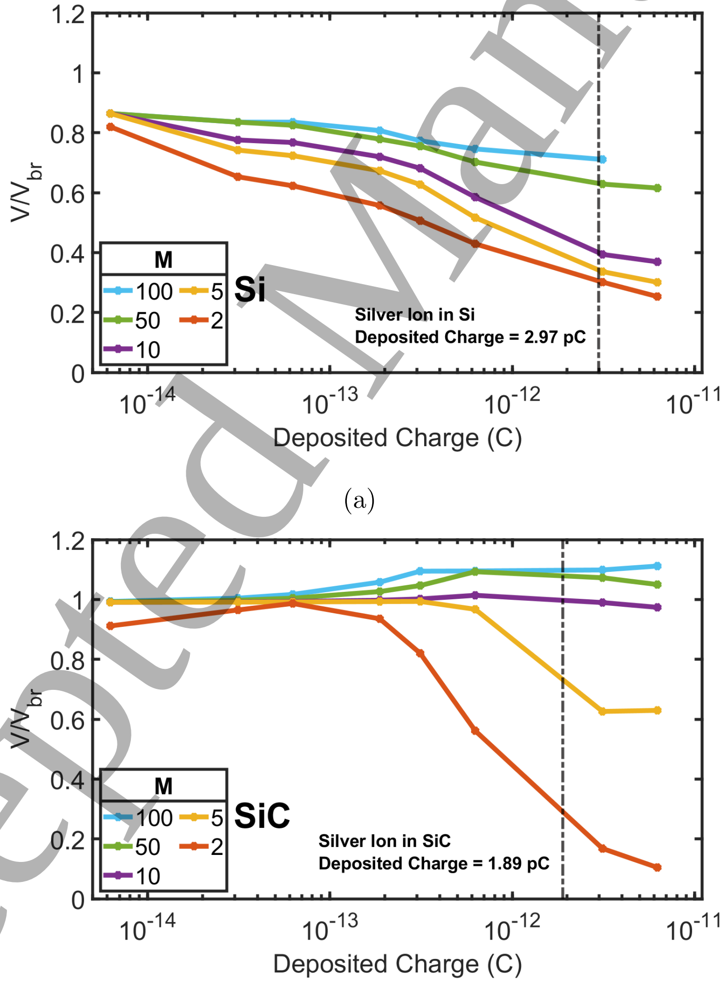

(a)

(b)

Figure 7. Charge multiplication after heavy ion transient : (a) Si and (b) SiC. The deposited charge from a Silver ion commonly used in SEE testing is displayed for both materials.

The data indicate the voltage for which a multiplication of M is achieved for a given heavy ion deposited charge. The ideal behaviour is that the lines would be flat with deposited charge - indicating that charge multiplication is insensitive to radiation. We see that this is largely the case for SiC, with only the voltage for small multiplications ($M = 2$ and 5) decreasing as the deposited charge increases. Further, we observe that M increases with deposited charge at higher voltages, indicating the device is more robust to failure. For the Si device it can be observed that at higher deposited charge a lower applied reverse bias is required to result in the same value of M being achieved. This indicates that the maximum allowable reverse bias for the Si device to be resistant to all of the heavy ion conditions simulated is 61% of the breakdown voltage. In contrast, the SiC device does not demonstrate charge multiplication values of 10, 50 and 100 for reverse bias values below the breakdown voltages, even for high deposited charge values. Further, for the SiC device a 60% reduction in cosmic ray sensitivity to the highest energy heavy ion impact simulated is shown when the $M = 10$ line is considered due to the higher bias required to result in this multiplication in comparison to the Si device.

However, the data in figure 7 show that for the $M = 2$ case for high levels of deposited charge, the Si device can operate at a higher reverse bias prior to resulting in the same charge multiplication value as for the SiC device. This condition may be considered an extreme limit for the simulations.

4. Conclusions

The radiation response of two materials key to the advancement of the future of the electrification of aircraft have been analyzed through heavy ion simulations. It has been found that over a range of aerospace specific operating conditions that SiC has reduced sensitivity to heavy ion interaction. Through this research and planned experimental testing focusing on device region sensitivity it is expected that the radiation response of complex SiC devices will be determined in the near future. From this, we will ensure that new devices for aerospace are robust to failure facilitating the step change in propulsion technology which is so urgently required to achieve major strides towards Net-Zero.

Acknowledgments

This work was supported by Rolls-Royce and Innovate UK as part of the SiCTAA project Grant Number 105104.

References

[1] Abbate C, Busatto G, Tedesco D, Sanseverino A, Silvestrin L, Velardi F and Wyss J 2019 *IEEE Transactions on Electron Devices* **66** 4235–4242 ISSN 15579646

[2] Hazdra P, Smrkovsky P, Vobecky J and Mihaila A 2021 *IEEE Transactions on Electron Devices* **68** 202–207 ISSN 15579646

[3] Albadri A, Schrimpf R, Galloway K and Walker D 2006 *Microelectronics Reliability* **46** 317–325

[4] Shoji T, Nishida S, Hamada K and Tadano H 2014 *Japanese Journal of Applied Physics* **53** 04EP03

[5] Casey M C, Lauenstein J M, Ladbury R L, Wilcox E P, Topper A D and LaBel K A 2015 *IEEE Transactions on Nuclear Science* **62** 2482–2489 ISSN 00189499

[6] Lauenstein J M 2018 *Microelectronics Reliability and Qualification Workshop (MRQW)* URL `https://aerospace.org/MRQW`

[7] Choyke W and Pensl G 1997 *MRS Bulletin* **22** 25–29 ISSN 0883-7694

[8] Schroder D K 2005 *Semiconductor Material and Device Characterization* (Hoboken, NJ, USA: John Wiley & Sons, Inc.)

[9] Kimoto T and Cooper J A 2014 *Fundamentals of Silicon Carbide Technology : Growth, Characterization, Devices and Applications.* (Singapore: Wiley)

[10] Henins I 1964 *Journal of research of the National Bureau of Standards. Section A, Physics and chemistry* **68A** 529–533 ISSN 0022-4332

[11] Bertuccio G and Casiraghi R 2003 *IEEE Transactions on Nuclear Science* **50** 175–185 ISSN 0018-9499

[12] Klein C A 1968 *Journal of Applied Physics* **39** 2029–2038 ISSN 0021-8979

[13] Synopsys 2020 Sentaurus Device User's Manual v. R-2020.09

[14] Javanainen A, Turowski M, Galloway K F, Nicklaw C, Ferlet-Cavrois V, Bosser A, Lauenstein J M, Muschitiello M, Pintacuda F, Reed R A, Schrimpf R D, Weller R A and Virtanen A 2017 *IEEE Transactions on Nuclear Science* **64** 2031–2037

[15] Lauenstein J M, Casey M C, Wilcox E P, Kim H and Topper A D 2013 Single-Event Effect Testing of the Cree C4D40120D Commercial 1200V Silicon Carbide Schottky Diode Tech. rep. URL `https://ntrs.nasa.gov/search.jsp?R=20170003887`

[16] Okuto Y and Crowell C R 1975 *Solid State Electronics* **18** 161–168 ISSN 00381101

[17] Hatakeyama T 2009 *physica status solidi (a)* **206** 2284–2294 ISSN 18626300

[18] Niwa H, Suda J and Kimoto T 2014 **778-780** 461–466

[19] Rees G J and David J P R 2010 *Journal of Physics D: Applied Physics* **43** 243001

[20] Lide D R 2003 *CRC Handbook of Chemistry and Physics, 84th Edition, 2003-2004* (Florida, USA: CRC Press)